

snow accumulation and annual runoff) is widely used as a measure of glacier response to climate variability and change. In cold, dry regions like the Canadian High Arctic, interannual variability in  $B_n$  is largely coupled to variability in mean summer temperature, while in more maritime regions like Iceland and southern Alaska, it is also affected by variability in winter precipitation.

As measurements for the 2009/10 balance year are not yet available, measurements are summarized here for 2008/09. These are available for twenty glaciers: three in Alaska, four in Arctic Canada, nine in Iceland, and four in Svalbard. Nineteen of the glaciers had a negative annual balance and only one (Dyngjökull in Iceland) had a positive balance. As predicted in last year's report (Sharp and Wolken 2010), measured mass balances were more negative than in 2007/08 in Svalbard, less negative in Iceland, and very negative in Alaska where, according to GRACE satellite gravimetry, the regional net balance for all Gulf of Alaska glaciers was  $-151 \pm 17 \text{ Gt yr}^{-1}$ , the most negative annual value in the GRACE record (A. Arendt and S. Luthcke 2011, personal communication). In Arctic Canada, surface mass balances of three of the four glaciers measured were among the six most negative balances in the 44- to 49-year record, extending the period of very negative balances that began in 1987.

The continued breakup of the floating ice shelves that fringe northern Ellesmere Island has been associated with recent warm summers. Large new fractures were detected in the Ward Hunt Ice Shelf on 7 and 14 August 2010, and further break up of the eastern part of the ice shelf was underway on 18 August. Some  $65 \text{ km}^2$ – $70 \text{ km}^2$  of the ice shelf was lost by the end of August (Sharp and Wolken 2010).

Data from the NCEP/NCAR R1 Reanalysis illustrate meteorological conditions over the major glaciated regions of the Arctic in the 2009/10 mass balance year (Table 5.1). Winter (September 2009–May 2010) precipitation was near normal (relative to the 1948–2008 mean) over many of the major glaciated regions of the Arctic outside Greenland, significantly above normal in Arctic Canada and Novaya Zemlya, and below normal in southern Alaska, consistent with April terrestrial snow depth anomalies (see section 5e4). Summer (June–August 2010) temperatures at 700 hPa were anomalously positive over a region including Iceland, Greenland, the Canadian Arctic, and northern Alaska, but anomalously negative over the Eurasian Arctic, especially over Novaya Zemlya (Table 5.1; see also Fig. 5.2d). This pattern is mirrored in that of 700 hPa geopotential height anomalies,

which were positive on the North American side of the Arctic and negative on the Eurasian side. Anomalous air flow associated with the positive geopotential height anomalies results in anomalous poleward-directed meridional winds over Davis Strait and Baffin Bay (see section 5b). These winds may be important in transporting heat to west Greenland and the Canadian Arctic from a region around southern Greenland, where summer sea surface temperature anomalies were  $+1^\circ\text{C}$  to  $+2^\circ\text{C}$ . The MODIS land surface temperature (LST) product provides a measure of the likelihood of summer melting on glaciers. In 2010, summer LST anomalies (relative to 2000–10) were positive in all glaciated regions of the Arctic, except Franz Josef Land, and very positive in the Canadian Arctic, where the average LST anomalies were  $+1.07^\circ\text{C}$  (Table 5.1).

By comparing 2009/10 meteorological conditions with those in 2008/09, and considering 2008/09 glacier mass balances, we predict that mass balances in 2009/10 were probably more negative than in the previous year in Arctic Canada and Iceland, less negative than in 2008/09 in southern Alaska, Svalbard, and Novaya Zemlya, and similar to those of 2008/09 in Severnaya Zemlya and Franz Josef Land.

*f. Greenland*—J. E. Box, A. Ahlström, J. Cappelen, X. Fettweis, D. Decker, T. Mote, D. van As, R. S. W. van de Wal, B. Vinther, and J. Wahr

#### 1) COASTAL SURFACE AIR TEMPERATURES

Record-setting high air temperatures were registered at all of the west Greenland long-term meteorological stations (Table 5.2). At Nuuk (Fig. 5.19), winter 2009/10 and spring and summer in 2010 were the warmest since 1873, when measurements began. At Prins Christian Sund, as at Nuuk, 2010 annual anomalies were three standard deviations above the 1971–2000 baseline. Warm anomalies were greatest at Aasiaat, where winter temperatures were  $7^\circ\text{C}$  above the 1971–2000 baseline, which is three standard deviations above the mean. Temperature anomalies extended west into Arctic Canada (see also section 5e5), but not into east and northeast Greenland.

These measurements are consistent with anecdotal data provided by a long-time resident of Greenland (2010, personal communication), who wrote on 4 February 2010: “we don’t have snow, we don’t have the cold” ... “This weather this year is really different, in 30 years that I live in Ilulissat, that is the first year in this conditions. We have lot of dog sledding tourists, but we cannot do the tour, too much ice on the hills and dangerous to drive by sled.” ... “no snow at all”.

**Table 5.1: Summer (June –August) 2010 700 hPa air temperature, winter (September 2009– May 2010) precipitation, and summer MODIS Land Surface Temperature (LST) anomalies for major glaciated regions of the Arctic (excluding Greenland). For ranks, 1 = year with highest summer air or land surface temperature and winter precipitation, and n is the number of years in the record. Air temperature and precipitation anomalies are relative to 1948–2008 climatology from the NCEP/NCAR R1 Reanalysis. Mean summer LST values are calculated from eight day averages of daytime, clear sky values for a period centered on 15 July of each year. The length of the measurement period varies between regions and is equal to the mean (+4 standard deviations) annual melt duration in each region during the period 2000–09 derived using microwave backscatter measurements from the Seawinds scatterometer on Quik-Scat. LST is measured for blocks of 1-km by 1-km cells containing only glacier ice centered on high elevation regions of major ice caps in each region. Block size varies with the size of the ice cap, but is consistent between years. LST anomalies are relative to the mean LST for the period 2000–10.**

Region	Sub-Region	Latitude (°N)	Longitude (°E)	2010 Jun–Aug 700hPa T Anomaly	2010 Rank	2009–10 Sep–May Ppt Anomaly	2009–10 Rank	2010 MODIS LST Anomaly	2010 Rank
				(°C)	(n=63)	(mm)	(n=62)	(°C)	(n=11)
<b>Arctic Canda</b>	N. Ellesmere Island	80.6–83.1	267.7–294.1	2.68	2	28.3	4	0.56	6
	Axel Heiberg Island	78.4–80.6	265.5–271.5	1.99	4	22.5	8	1.17	3
	Agassiz Ice Cap	79.2–81.1	278.9–290.4	2.03	4	55.8	9	1.34	2
	Prince of Wales Icefield	77.3–79.1	278–284.9	2.10	3	24.5	9	1.16	2
	Sydkap	76.5–77.1	270.7–275.8	2.11	1	57.3	8	1.28	2
	Manson Icefield	76.2–77.2	278.7–282.1	2.08	2	148.9	1	1.22	1
	Devon Ice Cap	74.5–75.8	273.4–280.3	1.96	2	19.9	16	1.02	1
	North Baffin	68–74	278–295	1.67	5	52.5	7	0.89	1
	South Baffin	65–68	290 – 300	1.65	5	-24.3	42	1.00	1
<b>Eurasian Arctic</b>	Severnaya Zemlya	76.25–81.25	88.75 – 111.25	-0.05	29	2.7	29	0.89	1
	Novaya Zemlya	68.75–78.75	48.75 – 71.25	-0.94-9	52	86.2	5	0.44	3
	Franz Josef Land	80–83	45 – 65	-0.01	32	-17	37	-0.06	7
	Svalbard	76.25–81.25	8.75 – 31.25	-0.30	44	16.9	23	0.49	2
	Iceland	63–66	338 – 346	1.62	2	-10	35	0.34	2
<b>Alaska</b>	SW Alaska	60–65	210 – 220	0.69	14	-29	36	0.38	3
	SE Alaska	55–60	220 – 230	0.57	17	-26	35	*0.53	2*

Later, the same source spoke of “10–12 days of” continuous “heat wave” like weather, in June, with “a lot of blue skies”. Ilulissat is at 69.0°N on the west coast of Greenland, ~100 km northeast of Aasiaat, and ~560 km north of Nuuk (see Fig. 5.19).

## 2) UPPER AIR TEMPERATURES

Seasonally-averaged 2010 upper air temperature data, available from twice-daily radiosonde observations (Durre et al. 2006), indicate a pattern of record-setting warm anomalies below 300 hPa (e.g., Fig. 5.19, inset). This is consistent with a warming trend prevailing since reliable records began in 1964 and especially since the mid-1980s (Box and Cohen 2006). Upper air temperature anomalies in 2010 are consistent among all stations, but, as at the surface stations, they are most pronounced in central-west Greenland (Table 5.2) and closest to normal in east Greenland.

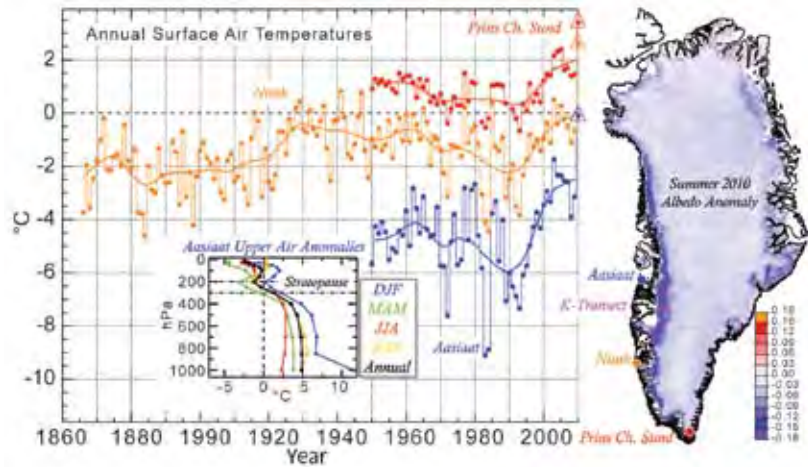


**FIG. 5.19.** Three Greenland meteorological station records illustrating the long-term time series of yearly-average temperatures. Triangles denote record-setting values, all in 2010. The inset shows upper air temperature anomalies in 2010 at Aasiaat relative to the 1971–2000 baseline. The map on the right shows summer (June–August) Greenland ice sheet surface albedo changes (from MODIS MODI0A1 data) and locations of meteorological stations and the K-Transect.

## 3) ATMOSPHERIC CIRCULATION

The high, positive temperature anomalies over the inland ice sheet are largely explained by atmospheric circulation anomalies. NCEP/NCAR Reanalysis data

<b>Table 5.2. 2009 Greenland station surface air temperature anomalies by season, relative to 1971–2000.</b>					
<b>Station (Region), Latitude, Longitude, time range</b>	<b>Winter</b>	<b>Spring</b>	<b>Summer</b>	<b>Autumn</b>	<b>Annual</b>
Thule AFB/Pituffik (NNW), 76.5° N, 68.8°W, 1961–2010	<b>4.1</b>	<b>2.6*</b>	<b>1.3</b>	2.4	<b>2.1*</b>
Upernavik (NW), 72.8°N, 56.2°W, 1873–2010	<b>6.1</b>	<b>4.0</b>	<b>1.4</b>	<b>2.8*</b>	<b>3.7*</b>
Aasiaat (W), 68.7°N, 52.8°W, 1951–2010	<b>7.1*</b>	<b>5.2*</b>	<b>1.5</b>	<b>2.5*</b>	<b>4.1*</b>
Nuuk (SW), 64.2°N, 43.2°W, 1873–2010	<b>5.4*</b>	<b>3.6</b>	<b>2.1*</b>	<b>3.3*</b>	<b>3.8*</b>
Prins Christian Sund (S), 60.0°N, 43.2°W, 1951–2010	<b>3.1*</b>	1.5	<b>1.8*</b>	<b>2.0*</b>	<b>2.3*</b>
Tasiilaq (SE), 65.6°N, 22.0°W, 1895–2010	<b>3.1</b>	0.8	<b>1.8</b>	<b>1.0</b>	<b>1.8</b>
Illoqqortoormiut (E), 70.4°N, 22.0°W, 1948–2010	0.3	-0.8	0.0	0.2	-0.1
Danmarkshavn (NE), 76.8°N, 18.8°W, 1949–2010	0.7	0.6	0.1	-0.4	0.0

\*Bold values indicate anomalies that meet or exceed one standard deviation from the mean. Underlined values exceed two standard deviations from the mean. Italicized values exceed three standard deviations from the mean. Asterisks indicate record-setting anomalies. Winter values include December of the previous year.

for 2010 indicate abnormally large heat flux from the south over the southwestern part of the Greenland ice sheet. NCEP/NCAR Reanalysis geopotential height anomalies at 500 hPa in June, July, and August 2010 (referenced to the 1971–2000 baseline) were at least twice the 1971–2000 standard deviation (see also section 5b.).

#### 4) SURFACE MELT EXTENT AND DURATION AND ALBEDO

The areal extent and duration of melting on the ice sheet, derived from daily passive microwave satellite remote sensing observations (Mote 2007), continued to increase in 2010. During April–September 2010 the melt area was ~8% more extensive than the previous record set in 2007 (Fig. 5.20). The 2010 melt extent through mid-September was 38% greater than the 1979–2007 average, and the June–August extent was 26% greater than the 1979–2007 average. Compared to summer 2007, when melt anomalies occurred in both the ablation and percolation zones (Tedesco et al. 2008), 2010 melt anomalies were concentrated in the lower elevation bare ice zone.

Abnormal melt duration was concentrated along the western margin of the ice sheet. This was consistent with the anomalous summer heat flux described above, preceded by abnormally high winter air temperatures that led to warm conditions prior to the onset of melt (Tedesco et al. 2011). The melt duration was as much as 50 days greater than average at elevations between 1200 and 2400 meters above sea level in west Greenland. In May, low elevation areas along the western ice margin melted for as much as 15 days longer than average.

The melt extent and duration observations are consistent with the observed coastal and upper air temperatures described above, and derived meteorological data. For example, NCEP/NCAR Reanalysis data suggest that May surface temperatures were up to

5°C above the 1971–2000 average. In June and August there were large positive degree day anomalies (up to 20 degree days) along the western and southern ice sheet. During August, temperatures were 3°C above average over most of the ice sheet, with the exception of the northeastern region. In August along the southwestern inland ice sheet, there has been an increase of 24 melting days during the past 30 years of passive microwave data coverage.

As melt extent and duration have increased during the last decade, MODIS10A1 data (Hall et al. 2006) indicate that the surface albedo of the ice sheet has also decreased, particularly along the western margin of the sheet (Fig. 5.19). The albedo decrease has been concentrated where bare ice has been exposed once the snow from the previous winter has melted away by mid-summer peak solar irradiance.

#### 5) SURFACE MASS BALANCE ALONG THE K-TRANSECT

The 150-km long K-Transect is located near Kangerlussuaq at 67°N between 340 m and 1500 m above sea level on the western flank of the ice sheet (van de Wal et al. 2005; Fig. 5.19). The surface mass balance between September 2009 and September 2010 was by far the lowest since 1990, when routine measurement began. Averaged over the length of the transect, the surface mass balance was 2.7 standard deviations below the 1990–2010 average. The altitude of the snow line, which describes the maximum areal extent of melting of the snow cover since the previous winter, was the highest on record, and a melt season that began very early (late April) continued until the beginning of September. Surface albedo values at the weather stations were below average and summer air temperatures were above average. In south Greenland, where the highest net ablation (~6 m of ice) of Greenland is found at low elevation, 2010 was unique in the observations since 1991, with about 9 m of ablation due to early melt and the lack of the commonly abundant winter precipitation, which usually takes one to two months to melt away.

The apparently strong link between negative surface mass balance and observed high air temperatures due to strong heat flux from the south and the record-high melt extent and duration, has been successfully simulated by the Modél Atmosphérique Régional (MAR) regional climate data assimilation model. It simulated an ice sheet surface mass balance 90% less positive than normal, the lowest net mass accumulation rate since 1958 when

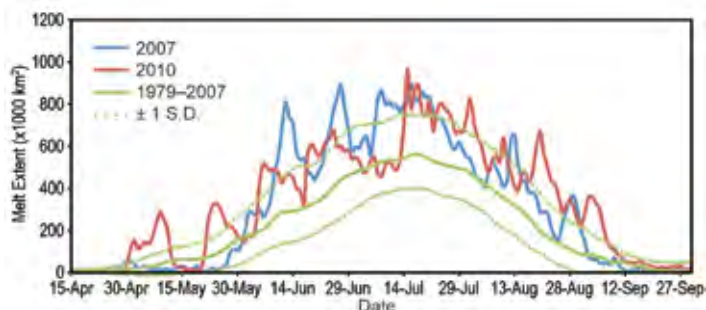


**FIG. 5.20. Time series of Greenland melt extent derived from passive microwave remote sensing. The broken green lines are ±1 standard deviation (S.D) of the 1979–2007 average. After Mote (2007).**

data to drive the model became available (Tedesco et al. 2011). This condition reflects a very heavy melt year combined with below-normal ice sheet snow accumulation.

### 6) TOTAL GREENLAND MASS LOSS FROM GRACE

GRACE satellite gravity solutions (Velicogna and Wahr 2006) are used to estimate monthly changes in the total mass of the Greenland ice sheet. For the hydrologic year 2009/10, i.e., from the end of the 2009 melt season, including October, through the end of October 2010, the ice sheet cumulative loss was -410 Gt, 177% (or two standard deviations) of the 2002–09 average annual loss rate of -231 Gt yr<sup>-1</sup>. The 2010 mass loss is equivalent to a eustatic sea level rise contribution of 1.1 mm. This was the largest annual loss rate for Greenland in the GRACE record, 179 Gt more negative than the 2003–09 average. The 2009/10 hydrological year ended 206 Gt more negative than the recent (2002–09) hydrological year average. Using GRACE data, Rignot et al. (2011) found an acceleration of Greenland ice sheet mass budget deficit during 1979–2010, in close agreement with an independent mass balance model.

### 7) MARINE-TERMINATING GLACIER AREA CHANGES

Marine-terminating glaciers are of particular interest because they represent the outlets through

which inland ice can move most quickly and in the largest quantities out to sea. Iceberg calving from these glaciers represents an area reduction and mass loss from the ice sheet, which contributes to sea level rise.

Daily surveys using cloud-free MODIS visible imagery (Box and Decker 2011; <http://bprc.osu.edu/MODIS/>) indicate that, during 2010, marine-terminating glaciers collectively lost a net area of 419 km<sup>2</sup>. This is more than three times the annual loss rate (121 km<sup>2</sup> yr<sup>-1</sup>) of the previous eight years, 2002–09 (Fig. 5.21). The calving of 290 km<sup>2</sup> of ice from Petermann Glacier ice shelf in far northwest Greenland accounted for 70% of the loss (see <http://bprc.osu.edu/MODIS/?p=69>). Glacier ice area loss elsewhere in 2010 (i.e., excluding Petermann Glacier) remained near the average loss rate of 121 km<sup>2</sup> yr<sup>-1</sup> observed since 2002. Glacier area change surveys (Howat and Eddy 2011) indicate that the ice area loss rate of the past decade is greater than loss rates since at least the 1980s.

A number of other large marine-terminating glaciers also lost a significant area of ice in 2010: Zachariae Isstrøm, northeast Greenland, 43 km<sup>2</sup>; Humboldt Glacier, northwest Greenland, 20 km<sup>2</sup>; Ikertivaq Glacier, Southeast Greenland, 15 km<sup>2</sup>; and five glaciers that flow into Upernavik glacier bay in northwest Greenland, 14 km<sup>2</sup>.

Since 2000, the net area change of the 39 widest marine-terminating glaciers is -1535 km<sup>2</sup> (17.5 times the size of the 87.5 km<sup>2</sup> Manhattan Island, New York) and the average effective glacier length change was -1.7 km. While the overall area change was negative, 7 of the 39 glaciers did advance in 2010 relative to 2009. The largest glacier area increases were at Ryder and Storstrømmen glaciers, 4.6 km<sup>2</sup> and 4.2 km<sup>2</sup>, respectively.

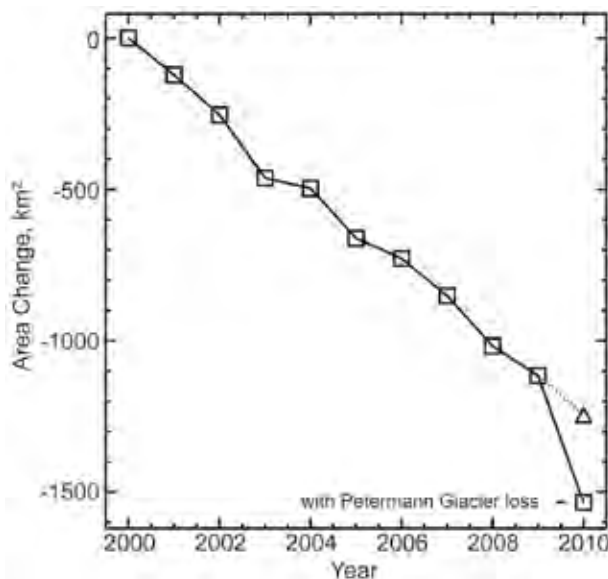


**FIG. 5.21. Cumulative net annual area changes for the 35 widest marine-terminating glaciers of the Greenland ice sheet. Net area change in 2010 is shown with and without the Petermann Glacier loss. The trend without the Petermann Glacier loss in 2010 is illustrated by the triangle and dashed line.**